Journal of Renewable Materials

Tech Science Press

DOI: 10.32604/jrm.2023.027441

ARTICLE

In Situ Generation of Copper Nanoparticles in Heat-Treated Copper-Containing Masson's Pine as a Preservative Process for Sawn Timber

Minting Lai, Guijun Xie*, Wanju Li, Lamei Li and Yongjian Cao

Guangdong Provincial Key Laboratory of Silviculture, Protection and Utilization, Guangdong Academy of Forestry, Guangzhou, 510520, China

*Corresponding Author: Guijun Xie. Email: xgj80@126.com

Received: 30 October 2022 Accepted: 30 November 2022

ABSTRACT

Heat-treated wood has good dimensional stability, durability, and color, but its susceptibility to fungal growth affects its commercial value. In this study, lumber harvested from mature Masson's pine (*Pinus massoniana* Lamb.) was vacuum impregnated with a basic copper salt solution (copper hydroxide, diethanolamine, and polyethylene glycol 200) prior to heat-treatment at 220°C for 3 h. Antifungal properties, surface chemistry, crystal structure and sugar contents were tested, compared with heat treatment alone. The results showed that the samples treated by heating without copper salt treatment showed poor suppression of fungal growth, the copper-impregnated heat-treated wood suppressed (100%) the growth of *Botryodiplodia theobromae* Pat., *Aspergillus niger* V. Tiegh., *Penicillium citrinum* Thom, and *Trichoderma viride* Pers. The combined results of X-ray photoelectron spectroscopy, X-ray diffraction and sugars analysis suggested that fungal inhibition by the heat-treated copper-bearing Masson's pine was mainly due to the reduction of the metal salt by PEG200 at high temperature to generate copper nanoparticles. In addition, the reduced sugar content of the treated timber, and hence the nutrient substrate for spoilage microbes, reduced in the presence of the metal salts at high-temperature. This study has demonstrated an effective method of increasing low-grade wood's utility and commercial value.

KEYWORDS

Heat treatment; Masson's pine; sawn timber; inhibition of fungal growth; copper nanoparticles

1 Introduction

Wood has good strength-to-weight and visual characteristics. Consequently, it is an important and widely used renewable resource. However, because wood is vulnerable to biological invasion and physical defects such as cracking and deformation, it is usually heat treated to improve its utility. High-temperature heat treatment is an attractive process that can improve the dimensional stability, durability, and color of wood [1–6]. Consequently, heat-treated wood products are popular materials and widely used in various settings such as decorative wallboard. Although heat-treated wood is generally considered to have good preservative properties, it can be susceptible to fungal growth [7,8].

The specialized extendible cells of fast-growing bamboo are expanded with sugar and water during growth, and the high nutrient content of its tissues promotes insect damage and microbial spoilage [9]. Because high temperatures can accelerate the modification of wood components, heat treatment can

influence changes in the fungal resistance properties of timber. Kamdem et al. [6] analyzed the decomposition resistance of heat-treated wood using improved soil block or agar block test methods and concluded that the decomposition resistance of heat-treated wood required improvement. Sivonen et al. [10] studied the spoilage of heat-treated pine (*Pinus spp*.) by brown rot fungus (*Coriolus versicolor*) and proposed that timber treated at a temperature above 220°C could attain high resistance to fungi. Zhu et al. [11] followed changes in the sugar contents of heat-treated wood from *Pinus spp.*, *Fraxinus mandshurica* and *Betula spp.* at 200°C, and found that the heat-treated wood was more prone to spoilage than the untreated control wood: When wood from *P. sylvestris* and *Betula spp*. was heat-treated at 180°C and 200°C, respectively, their sugar contents increased, and their contents in the surface layer were higher than that of core layer. In another study, heat treatment of timber from *P. sylvestris* var. *mongolica* and *Quercus mongolica* Fisch. At 185°C and 205°C respectively for 1.5 h, inhibited the damage caused by cyanobacteria, but did not inhibit or reduce surface fungal growth [7].

Nanomaterials impregnated wood can obtain better properties [12]. Photocatalytic nano-TiO_2 can partially inhibit *Aspergillus niger*, reduce the growth of harmful mold, and better protect wood-based artifacts [13]. However, *Pinus nigra* L. was treated by vacuum impregnation with nano zinc oxide, zinc borate and copper oxide, and the mildew test was carried out on three kinds of molds, namely *Aspergillus niger, Penicillium chrysogenum* and *Trichoderma viride*. It was found that nano zinc borate had a low control effect on mildew, and its infection value was 4, while the others had no control effect on mildew [14].

More recently, researchers have explored green methods by combining thermal modification with mineralization to improve the physico-mechanical properties and microbial resistance of wood. For example, wood impregnated with a silver nano-suspension (400 ppm) and heat-treated between 145°C and 165°C showed improvements in its physico-mechanical properties [15]. Xie et al. [16] impregnated wood samples with a copper-containing solution at high pressure, and the subsequent high-temperature treatment produced copper nanoparticles which have good antifungal properties.

Due to practical limitations, small sections of wood are often used in the research environment. However, wood is a naturally variable material, and studies of small specimens may not accurately reflect the behavior of the full-size material.

In this study, lumber from Masson's pine was impregnated with a basic copper salt solution and subjected to high-temperature treatment. Surface sections of the treated timber were tested to determine their antifungal properties, chemistry and crystal structure, and sugar contents using conventional methods. Large-size timber was chosen for the investigation to reduce the time between experimental research and production practice. Superior quality anti-mildew heat-treated wood can be obtained directly by cutting rough wood.

2 Materials and Methods

2.1 Materials

Wood was harvested from *P. massoniana* Lamb. (average diameter at breast height, 24 cm; average height, 16 m; age, 25 years) at the Xinyi Forestry Research Institute (Guangdong Province, China), and was without decay or microbial growth.

3,5-dinitrosalicylic acid (DNS), copper hydroxide, diethanolamine, glucose, polyethylene glycol 200 (PEG200), phenol, potassium sodium tartrate ($C_4H_4O_6KNa{\cdot}4H_2O$), sodium hydroxide, sodium metabisulfite ($Na_2S_2O_5$), were from Guangzhou, China. Arabinose, fucose, galactose, glucose, mannose, rhamnose, and xylose were purchased from Hubei Weishi Chemical Reagent Co., Ltd., China.

2.2 Preparation of Wood and Impregnation Solution

The timber was processed into six sawn sections measuring 600 mm × 220 mm × 30 mm shown in Fig. 1. The sections taken for analysis post-treatment are indicated by S1–S3 and CS1–CS3, which represent the different treatments applied (Table 1).

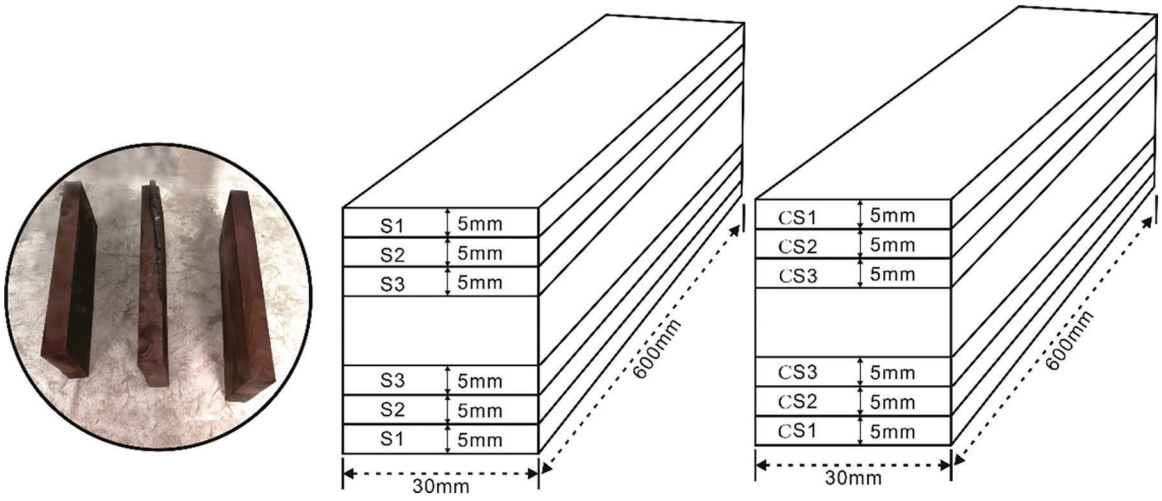

Figure 1: Dimensions of the lumber obtained from *P. massoniana* showing the sampling sections S1–S3 and CS1–CS3 (designating different treatments) taken for analysis post-treatment

Table 1: Experimental processing scheme for the heat-treated Masson's pine lumber (CS is non-impregnated control, S is the impregnated samples, 1–3 denotes the 5 mm sections taken for analysis)

Sample	Process		
	[CuG] (%)	θ heat treatment (°C)	t (h)
CS1	-	220	3
CS2	-	220	3
CS3	-	220	3
S1	6.35	220	3
S2	6.35	220	3
S3	6.35	220	3

The impregnation solution was composed of copper hydroxide, diethanolamine, polyethylene glycol 200 (PEG200) and water: Diethanolamine and copper hydroxide were mixed in a molar ratio of 2:1, and water was added with stirring until copper ammonia solution was formed, and then PEG200 is added to give the copper-containing impregnation solution (CuG).

2.3 Vacuum Impregnation

Freshly sawn timber samples were dried at 60°C to constant weight using a DHG-9051 kiln (Shanghai Bluepard Instruments Co., Ltd., China). Dried timber was then immersed in the CuG solution contained in a vacuum dipping tank (Self-Assembled Equipment, China) maintained at −0.09 MPa for 30 min, followed by 1.5 MPa for 40 min. Following treatment, the timber was dried to a constant weight at 60°C in the kiln.

2.4 Heat Treatment

Vacuum impregnated timber was heat treated in a customized (Jiangxi Meilong Wood Protection Co., Ltd., China) vacuum steam chamber under the following conditions: Steam treatment at 100 kPa for 20 min; thermal (electric) heat treatment at 220°C for 3 h; controlled cooling to 140°C under steam.

2.5 Processing Sequence for Masson's Pine Lumber

The sequence of processing treatments for the Masson's pine lumber is given in Table 1.

2.6 Fungal Inhibition Test

The fungal resistance of the treated samples was determined by the method given in Chinese standard GB/T 18261–2013 using *Botryodiplodia theobromae* Pat., *Aspergillus niger* V. Tiegh., *Penicillium citrinum* Thom and *Trichoderma viride* Pers., which were all purchased from the Chinese General Microbiological Culture Collection Center (Beijing, China). The test was repeated six times for each set of samples. Briefly, culture medium (2% maltose and 1.5% agar) was inoculated with the chosen fungal strain and cultivated at 28°C and 85% relative humidity for 7 d. Two sterilized glass rods were placed the culture medium, followed by the sterilized wood samples to be tested. After one month, the discoloration grade (0–4) of the wood sample was recorded: 0, no mold growth; 1, mold area < 25%; 2, mold area 25%–50%; 3, mold area between 50%–75%; 4, mold area > 75%. The efficacy of fungal growth control (E) was calculated from Eq. (1).

$$E = \left(1 - \frac{D_1}{D_0}\right) \times 100\% \tag{1}$$

where D_1 is the average discoloration grade, and D_0 is the average discoloration grade of the control sample.

2.7 Scanning Electronic Microscopy (SEM) and Energy Dispersive Spectroscopy (EDS)

The heat-treated copper-bearing wood samples were ground into powders that were subsequently analyzed using SEM (Zeiss SUPRA 40, Oberkochen, Germany) and EDS (ZEISS SUPRA 40).

2.8 X-Ray Photoelectron Spectroscopy (XPS)

Two samples from each treatment group were selected at random, and reduced to a fine powder using a 425 and a 250 μm sieve, and a 20 mg aliquot was analyzed using an Escalab 250XI Instrument (Thermo Fisher Scientific, USA).

2.9 X-Ray Diffraction Analysis (XRD)

The crystal form and particle size of the metal species were characterized using powdered samples (100 mg, see above) on a D8 diffractometer (Bruker, USA).

2.10 Analysis of Sugars

2.10.1 Sample Extraction

Samples of powdered wood (1.5 g) were combined with distilled water (30 mL) in a hydrolysis bottle, shaken at 50°C for 0.5 h, quickly filtered, and the filtrate (2 mL) taken for the analysis of total reducing sugars and total sugars.

2.10.2 Total Reducing Sugars

DNS (7.5 g) and sodium hydroxide (14.0 g) were dissolved in hot water (1000 mL; added 10 min after boiling) and allowed to cool. Potassium sodium tartrate (216.0 g, phenol (5.5 mL, melted in a water bath at 50°C) and sodium metabisulfite (6.0 g) were then added, and the solution was stored in an amber glass bottle and used within 5 d.

Glucose reference standard was dried at 105°C for 3 h and used to prepare a stock standard solution (100 mL of 1 g L^{-1}) in distilled water. Glucose calibration standards were prepared over 0.2–0.02 mg mL^{-1} from aliquots of the stock standard solution according to the dilutions given in Table 2.

To each calibration standard or sample extract (2 mL), contained in 25 test tubes, DNS (1.5 mL) was added, shaken to mix, and incubated in boiling water for 5 min. The absorbance of the cooling solutions was recorded at 520 nm. The amounts of reducing sugars in the samples were obtained from the absorbance/glucose mass standard curve.

Table 2: Glucose calibration standards: Stock standard solution (1 mg L^{-1}) dilutions

Target concentration (g L^{-1})	Dilution factor	Volume of stock standard (mL)	Added water (mL)
0.20	5.00	1.0	4.00
0.18	5.55	1.0	4.55
0.16	6.25	1.0	5.25
0.14	7.14	1.0	6.14
0.12	8.33	1.0	7.33
0.10	10.00	1.0	9.00
0.08	12.50	1.0	11.50
0.06	16.66	0.5	7.83
0.04	25.00	0.5	12.00
0.02	50.00	0.2	9.80

2.10.3 Total Sugars

A glucose stock standard solution (2 mg L^{-1}), prepared from the dried reference material above, was used to prepare calibration standards over 0.1–0.02 mg L^{-1} according to the dilutions given in Table 3.

Table 3: Total sugars glucose calibration standards: Stock standard solution (2 mg L^{-1}) dilutions

Target concentration (g L^{-1})	Dilution factor	Volume of stock standard (mL)	Added water (mL)
0.20	10.00	0.50	4.50
0.18	11.11	0.50	5.05
0.16	12.5	0.50	5.75
0.14	14.29	0.50	6.64
0.12	16.67	0.50	7.83
0.10	20.00	0.40	7.90
0.08	25.00	0.30	7.20
0.06	33.33	0.20	6.47
0.04	50.00	0.10	4.90
0.02	100.00	0.09	8.91

To each calibration standard or sample solution (2 mL), contained in 25 mL glass tubes, sulfuric acid (5.0 mL) was added dropwise, shaken to mix, and incubated at 50°C for 30 min. The absorbance of cooling solutions was recorded at 490 nm, and the total sugar contents of the samples were obtained from the absorbance/glucose mass standard curve. Distilled water was used as the blank control.

2.10.4 Analysis of Individual Reducing Sugars by LC-MS

A mixed stock standard solution of each monosaccharide (rhamnose, fucose, xylose, arabinose, glucose, mannose, galactose), prepared at 50 mg mL^{-1} in deionized water (4 mL), was serially diluted to given calibrations standards over the range 5–500 ppm; solutions were passed through a 0.22 μm membrane filter prior to LC-MS.

Powdered wood extracts (2 mL) were vacuum dried at 50°C to near dryness, reconstituted with deionized water (1 mL), and passed through a membrane syringe filter (0.22 um) prior to analysis by LC-MS.

Calibration standards and sample extracts were analyzed with a LCMS8040 LC/MS system (Shimadzhu, Tokyo, Japan). Sugars in the injection solutions (2 μL) were separated on an InertSustain NH2 column (5 um, 4.6 mm × 250 mm; GL Sciences (Shanghai) Ltd., China) maintained at 35°C: The analytical column was protected by an InertSustain NH2 guard column (5 um, 4.0 mm × 10 mm); the mobile phase was 25% water 75% acetonitrile using isocratic elution at 1.1 ml min^{-1}. Eluting sugars were ionized in the ESI source operating at 3.5 KV, and atomizing and drying gas flow rates of 3 and 15 L min^{-1}, respectively. The desolvation line and heating module temperatures were 250°C and 400°C. Monosaccharide precursor to product ion transitions was recorded in the negative ion multiple reaction monitoring (MRM) mode at a collision energy of 35 eV.

3 Results and Discussion

3.1 Antifungal Properties of Heat-Treated Masson's Pine

The control materials (CK, no treatment), and heat-treated timber with copper (S1–S3) and without copper (CS1–CS3) exhibited different inhibitory effects towards each fungal species (Fig. 2). As expected, CK prepared with each treatment group exhibited no inhibition, thereby confirming the validity of the test results (Figs. 2A, 2H).

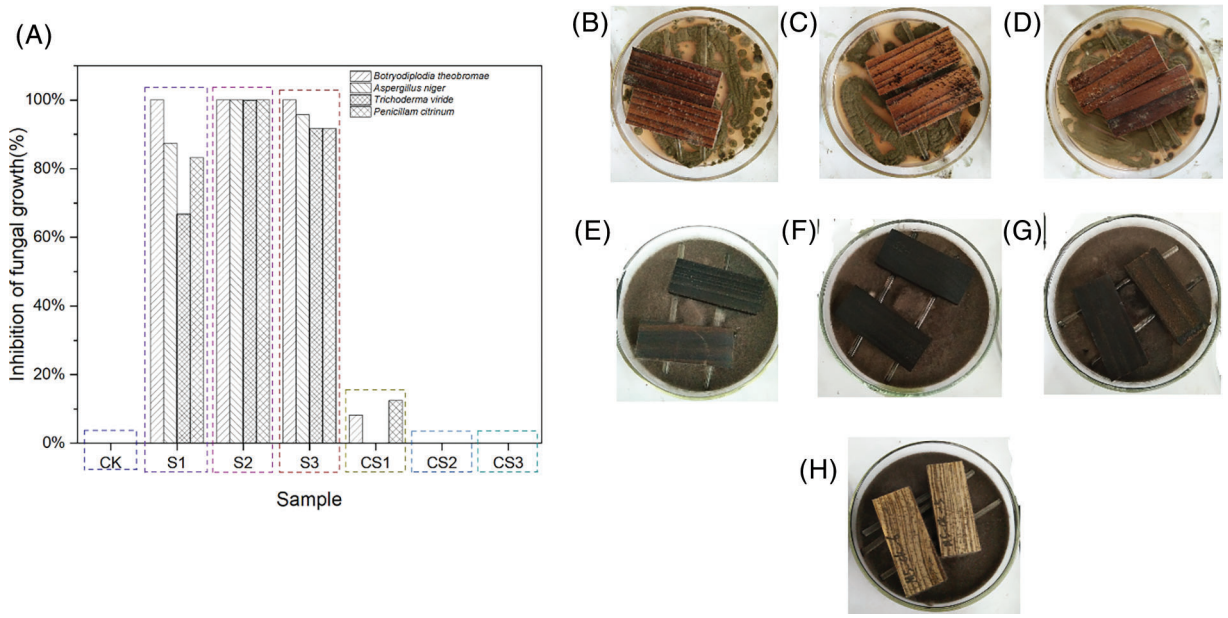

Figure 2: Inhibition of fungal growth by treated Masson's pine lumber (A). Photographs that are some examples show inhibitory zone of the prepared wood against *Aspergillus niger* V. Tiegh. and *Trichoderma viride* Pers. for four weeks. In which CS1 (B), CS2 (C), CS3 (D), S1 (E), S2 (F), S3 (G), CK (H)

Sections of the heat-treated lumber (CS1–CS3) showed some inhibition towards *Botryodiplodia theobromae* Pat. (8.25%) and *Penicillium citrinum* Thom (12.55%) only, while CS2 and CS3 had no inhibition activity. In contrast, all surface sections of the heat-treated copper-bearing Masson's pine (S1–S3) exhibited good inhibition properties: 67%–100% for S1; 100% for S2; and 92%–100% for S3: the lowest antifungal activity was observed for S1 towards *Trichoderma viride* Pers. (67%).

3.2 SEM, EDS and Surface Chemistry (XPS)

Fig. 3 shows the SEM and EDS test results of heat-treated copper-containing Masson's pine lumber (S) and untreated Masson's pine control wood (CK). On the whole, the inner surface of CK is relatively smooth. After heat treatment, the inner surface of Cu-impregnated Masson's pine wood was rough with many small cracks by SEM photos, and copper element was observed on the inner surface by EDS photos. Among them, EDS shows that S2 has the strongest copper signal, which is as well as the work reported by Aguayo et al. [12], corresponding to the best mildew resistance in Section 3.1, which supports that copper in wood can inhibit the growth of mold.

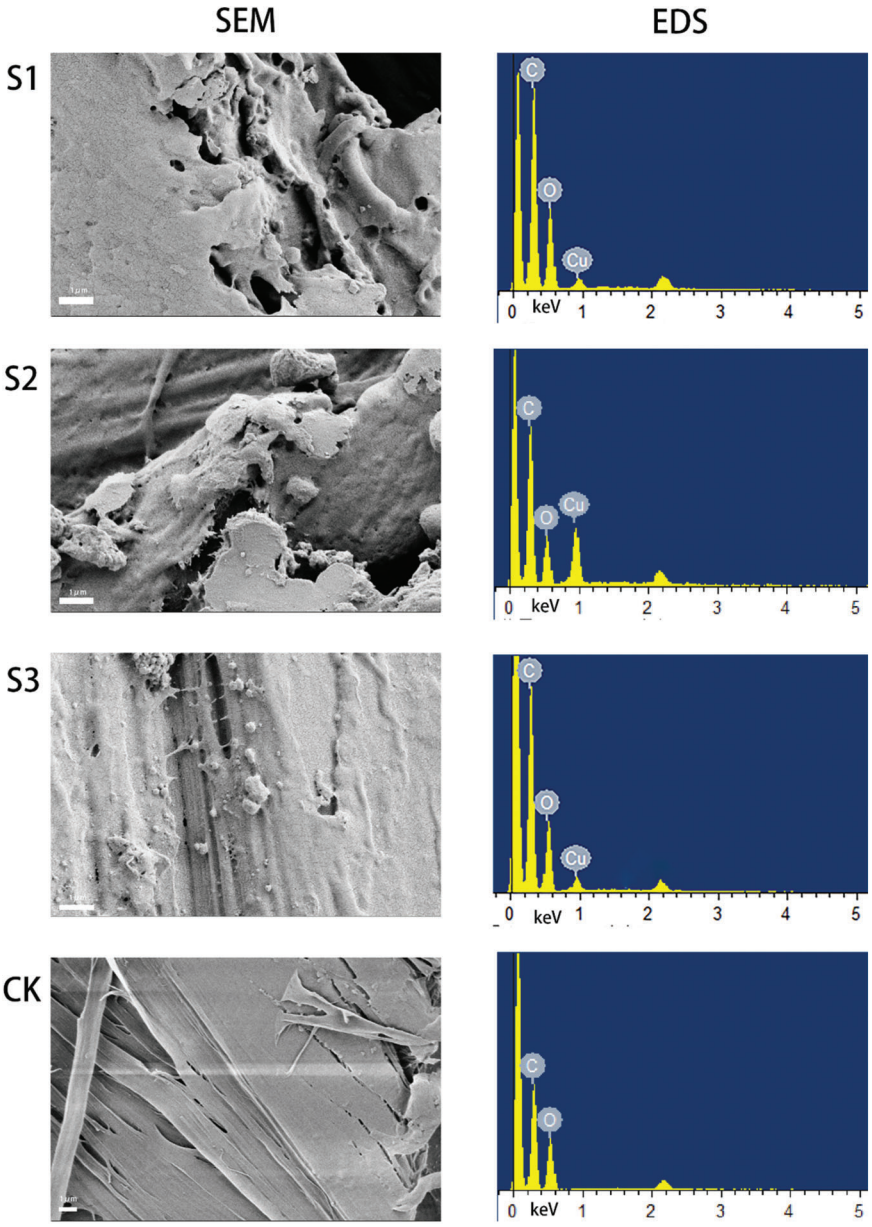

Figure 3: SEM and EDS results for heat-treated wood samples dipped in solutions of copper. S is the impregnated samples, 1–3 denotes the 5 mm sections taken for analysis. CK is the samples with no treatment

The C1 S peaks of wood fiber can usually be deconvoluted into four peaks (C1, C2, C3 and C4; Table 4): C1 can be assigned to lignin and surface contamination; C2 is largely due to carbon atoms in cellulose; C3 mainly arises from oxidation products containing ketone and aldehyde groups, or from the cellulose molecules within lignin; C4 is due to the carbonyl group attached to a heteroatom [17,18].

Table 4: Peak assignments for XPX C1s and O1s in wood [17]

Peak	Binding energy (eV)	Symbol	Assignment
C1s	285 ± 0.4	C1	C–C, C–H
	286.5 ± 0.4	C2	C–OH, C–O–C
	288.0 ± 0.4	C3	C=O, O–C–O
	289.0 ± 0.4	C4	O–C=O
O1s	533.0 ± 0.4	O1	C–O, C–O–C, O–C=O, C=O

Fig. 4 shows the high-resolution XPS C1s obtained from the heat-treated copper-bearing lumber. The absence of C4 differed from literature reports [17–19]: The peak at 285.0 eV agreed with reported values for the binding energy of C1 (284.6–285.0 eV) [19,20], and was attributed to the C–C bonding; 286.5 eV was assigned to C2, and may be due to C–O bonds [21]; 288.0 eV agreed with C3, and a C=O structure was inferred. A peak due to C4 was not observed, indicating that its content was very small [22].

The XPS spectra of Cu 2p from the heat-treated copper-bearing samples (S1–S3) are shown in Fig. 4B: The peaks between 932.8 and 952.3 eV, were assigned to Cu0; while the peak between 934.2 and 954.4 eV agreed with Cu^{+}. This suggested that divalent copper ions undergo bond cleavage or reduction reactions during heating and are reduced to Cu0 and Cu^{+}. Because the heat-treatment conditions for the lumber (220°C, 3 h) were below the thermal decomposition properties of the copper salt ($Cu(OH)_2$), this indicated that high-temperature bond cleavage was unlikely. However, residual PEG200 (from the CuG) can initiate the reduction of Cu^{2+} in wood, generating Cu0 and some Cu^{+} [23,24].

The XPS N1S spectra suggested the presence of amino groups arising from the wood and introduced in the pretreatment process (Fig. 3C). The single peak in the O1S spectra implied that there is only one O state in the heat-treated copper-containing Masson's lumber (Fig. 4D).

Table 5 gives the surface chemical composition of the untreated control and treated samples measured by XPS. The observed decrease in the O/C ratios for CS1–CS3 agreed with a decrease in the carbohydrate content with increasing surface depth in the lumber [25], probably due to their migration to the surface with the movement of water during heating [26].

The relative C1s peak intensities of the untreated control and treated Masson's pine lumber are given in Table 6. Compared with CK, the intensity of the C1s peaks in S1 showed the following trend: C1 decreased from 55.8% to 39.0%; C2 increased from 32.2% to 56.5%; C3 decreased from 6.5% to 4.6%, and C4 disappeared. The decrease in C1 and simultaneous increase in C2 peak intensities implied an increase in OH groups in the surface layer, which would facilitate the adsorption of water vapor from the air. The antifungal effects of heat-treated copper-bearing Masson's pine were much higher than that of CK, which could be attributed to the in situ Cu0 and Cu^{+}. The intensity of the C1S peaks showed the following trends with increasing surface depth (S1–S3): C1 decreased and increased: C2 and C3 both increased and decreased. Since the sawn section of S2 exposes more cellulose to the atmosphere, the increased oxygen functionality also increases the wettability of the material. However, increased wettability enhances the antifungal properties of the copper nanoparticles [27].

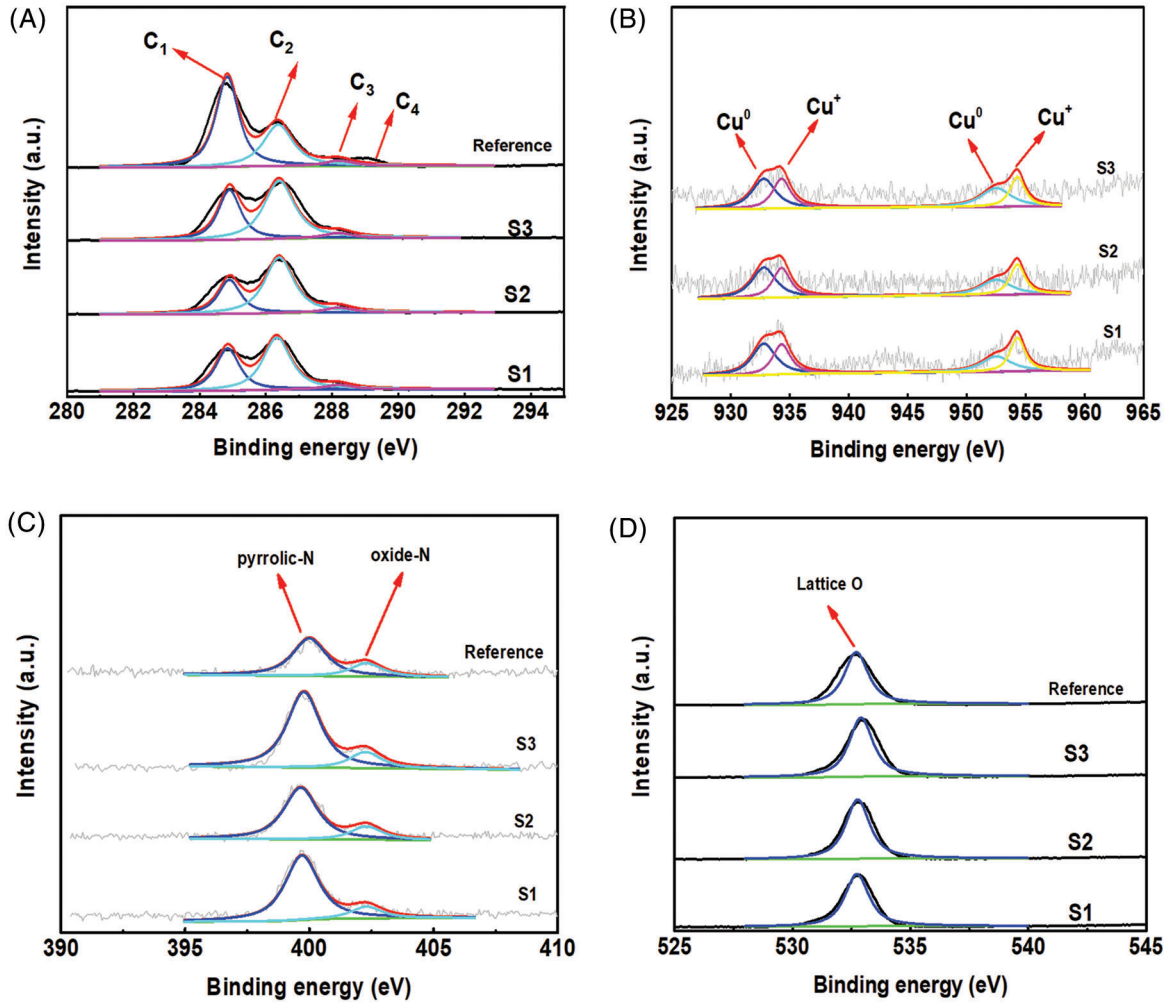

Figure 4: High resolution XPS spectra of copper-containing heat-treated wood. (A) C1s spectra, subpeak separated by deconvolution. (B) Cu spectra. (C) N spectra. (D) O1s spectra

Table 5: Surface chemical composition of the untreated control and treated samples measured by XPS

Samples	Surface composition (atom %)			
	C	O	O/C	Cu
CK	53.71	46.29	0.86	/
CS1	44.02	55.98	1.27	/
CS2	48.07	51.93	1.08	/
CS3	50.34	49.66	0.99	/
S1	44.28	50.94	1.15	4.78
S2	40.92	54.69	1.34	4.39
S3	45.59	50.19	1.10	4.22

Table 6: Relative C1s peak intensities, calculated from the XPS spectra of untreated control and treated Masson's pine lumber

Sample	Relative C1s peak intensities (%)			
	C1 (285 eV)	C2 (286.5 eV)	C3 (288 eV)	C4 (289 eV)
CK	55.8	32.2	6.5	5.5
CS1	46.4	49.1	4.5	-
CS2	50.8	44.8	4.4	-
CS3	57.2	39.1	3.7	-
S1	39.0	56.5	4.6	-
S2	30.5	64.1	5.4	-
S3	37.0	58.3	4.7	-

3.3 Crystalline Structure (XRD)

Fig. 5 shows the XRD patterns obtained from the analysis of heat-treated and heat-treated copper-containing Masson's pine lumber. The absence and presence of peaks due to Cu crystals in samples CS1–CS3 and S1–S3 respectively agreed with the XPS analysis (Table 5). Cu0 and Cu1 (Cu_2O), identified by high-resolution XPS, can both form crystal structures. However, the peaks at 43.29°, 50.51° and 74.15° correspond to the (111), (200), and (220) planes of CuO, which conformed to PDF#065-9026 for copper and a centered cubic crystalline structure. However, Cu_2O did not appear to form crystal structures in the treated wood, or it formed too few to be observed. The results differed from a similar investigation that involved the hydrothermal carbonization of wood containing zinc ions, which showed no change in the oxidation state of the metal [28]. In this study, the presence of residual PEG200 induced the reduction of Cu^{2+} to Cu^{+} and Cu0 during hydrothermal carbonization [29], where the average particle size of the crystalline copper particles was 100 nm [30].

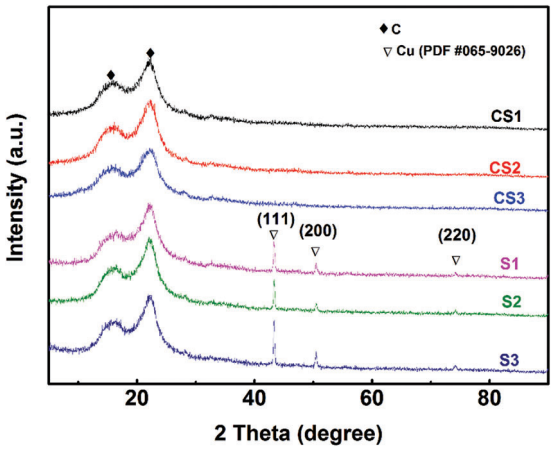

Figure 5: XRD patterns obtained from the heat-treated, and heat-treated copper-containing lumber

3.4 Sugar Profiles

There is a correlation between the sugar content of wood and the mildew-prone property of wood. The mechanism of wood mildew can be inferred by studying the changes in the sugar content of wood after heat treatment [31].

Fig. 6 shows the total sugar and total reducing sugar contents in the untreated and treated Masson's pine samples. Total sugars measurement refers to the water-soluble mono- and disaccharides. Reducing sugars comprise the aldose and ketose saccharides which convert to the open-chain form with an aldehyde group, e.g., mainly glucose, fructose, xylose, arabinose, etc.

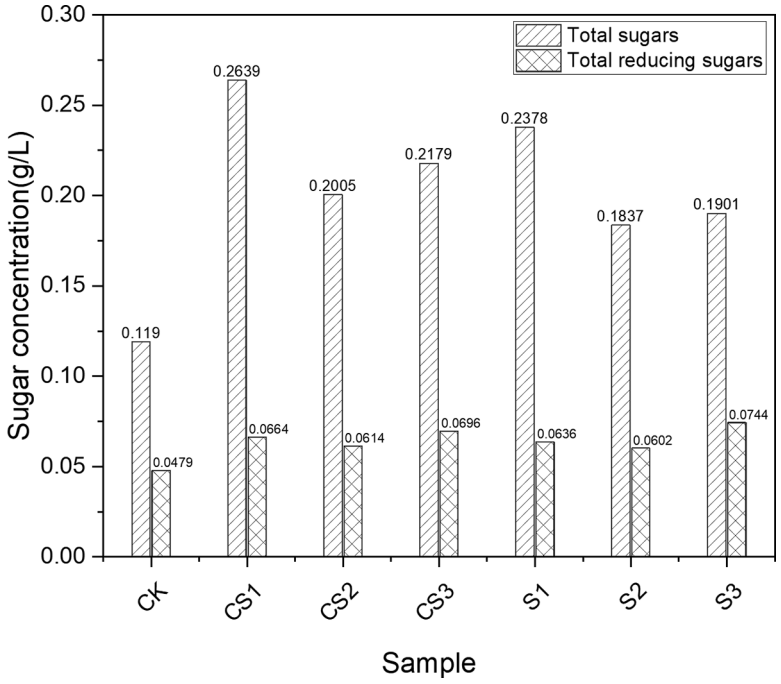

Figure 6: Total sugars and total reducing sugar contents of samples taken from the treated Masson's pine lumber

The total sugars and total reducing sugar contents of samples taken from the treated Masson's pine lumber are shown in Fig. 6. Compared with CK, the total sugars and total reducing sugars were all higher in the treated samples. Among the treated samples, the lowest and highest total sugar contents were measured in S2 and S1, respectively, which agreed with the results from the fungal control experiments (Fig. 2). The relatively low concentrations of reducing sugars may also account for the reduction of Cu^{2+} to Cu^{+}, and the low detectability of the monovalent ion [32].

Table 7 shows the concentrations of individual reducing sugars in the untreated and treated Masson's lumber obtained using LC-MS: Arabinose, and glucose + mannose (34.25–30.96 μg g^{-1}) were found in CK; small amounts of xylose, and glucose + mannose (0.64–1.82 μg g^{-1}) were present in S1–S3; and xylose and arabinose (2.33–9.33 μg g^{-1}) were present in CS1–CS3. A previous study showed that the content of arabinose gradually increases from sapwood to heartwood, while xylose is related to hemicellulose [33]. Thermal degradation of hemicellulose may lead to the formation of xylose in the Masson's pine lumber. Since xylose and arabinose are degraded at temperatures above 220°C, their contents increase with increasing depth in the surface layers of after heat treatment [34,35]. The trace amounts of xylose, and glucose + mannose in the S1–S3 could be attributed to their increased degradation by metal salts in the wood.

Overall, the results showed that the sugar content of heat-treated wood was much higher than that of its copper-bearing counterpart. Hence CS1–CS3 were more susceptible to fungal growth.

Table 7: Individual reducing sugar contents of untreated and treated Masson's lumbar measured by LC-MS

Sample	Sugar (μg g^{-1})						
	Rhamnose	Fucose	Xylose	Arabinose	Glucose + mannose	Galactose	Sum
CK	/	/	/	34.25	30.96	/	65.21
S1	/	/	/	/	/	/	/
S2	/	/	0.64	/	/	/	0.64
S3	/	/	/	/	1.82	/	1.82
CS1	/	/	2.33	4.65	/	/	6.98
CS2	/	/	2.68	7.01	/	/	9.69
CS3	/	/	3.52	9.33	/	/	12.85

4 Conclusion

The heat-treated copper-bearing Masson's pine lumber samples, after removing the surface layer, showed good antifungal properties: The middle surface layer (5–10 mm) totally suppressed (100%) the growth of *Botryodiplodia theobromae* Pat., *Aspergillus niger* V. Tiegh., *Penicillium citrinum* Thom, and *Trichoderma viride* Pers. The equivalent samples subjected to heat treatment alone showed virtually no inhibition of fungal growth (0%–12.5%). The antifungal properties of the heat-treated of copper-containing lumber could be attributed to two processes: i) The reduction of residual copper salts from the impregnation process by PEG200 at high temperature to generate antifungal copper nanoparticles; ii) the degradation of reducing sugars influenced by metal salts during heat treatment. Hence, the immersion of timber in a CuG dipping solution followed by high-temperature treatment may be an effective method of increasing the utility and value of low-grade lumber.

Acknowledgement: The authors would like to express their gratitude to EditSprings (https://www.editsprings.cn) for the expert linguistic services provided.

Funding Statement: This research was sponsored by the Guangdong Forestry Science and Technology Innovation Project "Research on the Thermal Modification of Eucalyptus and Spingbract Chinkapin Wood and the Key Technologies of Their Wood Flooring Preparation" (No. 2018KJCX006).

Conflicts of Interest: The authors declare that they have no conflicts of interest to report regarding the present study.

References

1. Zhan, T., Zhu, J., Liu, Z., Li, T., Peng, H. et al. (2022). Meta-analysis of chromatic properties of heat-treated wood. *European Journal of Wood and Wood Products, 80,* 851–858. https://doi.org/10.1007/s00107-022-01831-5
2. Zhan, T., Liu, Z., Peng, H., Jiang, J., Zhang, Y. et al. (2021). Meta-analysis of anti-swelling efficiency (ASE) of heat-treated wood. *European Journal of Wood and Wood Products, 79(4),* 1031–1034. https://doi.org/10.1007/s00107-021-01691-5
3. Paes, J. B., Brocco, V. F., Loiola, P. L., Segundinho, P. G. A., Silva, M. R. (2021). Effect of thermal modification on decay resistance of corymbia citriodora and pinus taeda wood. *Journal of Tropical Forest Science, 33(2),* 185–190. https://doi.org/10.26525/jtfs2021.33.2.185
4. Esteves, B., Marques, A. V., Domingos, I., Pereira, H. (2007). Influence of steam heating on the properties of pine (*Pinus pinaster*) and eucalypt (*Eucalyptus globulus*) wood. *Wood Science and Technology, 41(3),* 193–207. https://doi.org/10.1007/s00226-006-0099-0

5. Wang, J. Y., Cooper, P. A. (2005). Effect of oil type, temperature and time on moisture properties of hot oil-treated wood. *Holz als Rohund Werkstoff, 63(6),* 417–422. https://doi.org/10.1007/s00107-005-0033-4
6. Kamdem, D. P., Pizzi, A., Jermannaud, A. (2002). Durability of heat-treated wood. *Holz als Rohund Werkstoff, 60(1),* 1–6. https://doi.org/10.1007/s00107-001-0261-1
7. Gu, L. B., Ding, T., Lu, B., Zhu, K. (2010). Study on biological durability of pressurized steam-treated wood. *China Forest Products Industry, 37(5),* 6–9. https://doi.org/10.3724/SP.J.1011.2010.01351
8. Goffredo, G. B., Citterio, B., Biavasco, F., Stazi, F., Barcelli, S. et al. (2017). Nanotechnology on wood: The effect of photocatalytic nanocoatings against *Aspergillus niger*. *Journal of Cultural Heritage, 27,* 125–136. https://doi.org/10.1016/j.culher.2017.04.006
9. Mantanis, G., Terzi, E., Kartal S, N., Papadopoulos, A. N. (2014). Evaluation of mold, decay and termite resistance of pine wood treated with zinc- and copper-based nanocompounds. *International Biodeterioration & Biodegradation, 90(4),* 140–144. https://doi.org/10.1016/j.ibiod.2014.02.010
10. Sivonen, H., Nuopponen, M., Maunu, S. L., Sundholm, F., Vuorinen, T. (2003). Carbon-thirteen cross-polarization magic angle spinning nuclear magnetic resonance and Fourier transform infrared studies of thermally modified wood exposed to brown and soft rot fungi. *Applied Spectroscopy, 57(3),* 266–273. https://doi.org/10.1366/000370203321558164
11. Zhu, K., Cheng, K. H., Hui-Ming, L. I., Chen, R. W., Shao, Y. P. (2010). Mold inhibition of heat-treated lumber. *China Wood Industry, 24,* 42–44. https://doi.org/10.19455/j.mcgy.2010.01.013
12. Aguayo, M. G., Erazo, O., Montero, C., Reyes, L., Gacitúa, W. et al. (2022). Analyses of impregnation quality and mechanical properties of radiata wood treated with copper nanoparticle- and micronized-copper-based wood preservatives. *Forests, 13,* 1636. https://doi.org/10.3390/f13101636
13. Ahmed S, A., Yang, Q., Sehlstedt-persson, M., Morén, T. (2013). Accelerated mold test on dried pine sapwood boards: Impact of contact heat treatment. *Journal of Wood Chemistry & Technology, 33(3),* 174–187. https://doi.org/10.1080/02773813.2013.773041
14. Yang, K., Li, X., Wu, Y., Zheng, X. (2021). A simple, effective and inhibitor-free thermal treatment for enhancing mold-proof property of bamboo scrimber. *European Journal of Wood and Wood Products, 79(5),* 1049–1055. https://doi.org/10.1007/s00107-021-01655-9
15. Taghiyari, H. R., Bayani, S., Militz, H., Papadopoulos, A. N. (2020). Heat treatment of pine wood: Possible effect of impregnation with silver nanosuspension. *Forests, 11(4),* 466. https://doi.org/10.3390/f11040466
16. Xie, G., Zhou, Y., Cao, Y., Li, L. (2018). Anti-mildew properties of copper cured heat-treated wood. *BioResources, 13(3),* 5643–5655. https://doi.org/10.15376/biores.13.3.5643-5655
17. Nzokou, P., Pascal Kamdem, D. (2005). X-ray photoelectron spectroscopy study of red oak-(*Quercus rubra*), black cherry-(*Prunus serotina*) and red pine-(*Pinus resinosa*) extracted wood surfaces. *Surface and Interface Analysis, 37(8),* 689–694. https://doi.org/10.1002/sia.2064
18. Kamdem, D. P., Riedl, B., Adnot, A., Kaliaguine, S. (1991). ESCA spectroscopy of poly (methyl methacrylate) grafted onto wood fibers. *Journal of Applied Polymer Science, 43(10),* 1901–1912. https://doi.org/10.1002/a1991.070431015
19. Inari, G. N., Petrissans, M., Lambert, J., Ehrhardt, J. J., Gerardin, P. (2006). XPS characterization of wood chemical composition after heat-treatment. *Surface and Interface Analysis, 38(10),* 1336–1342. https://doi.org/10.1002/sia.2455
20. Barry, A. O., Koran, Z., Kaliaguine, S. (1990). Surface analysis by ESCA of sulfite post-treated CTMP. *Journal of Applied Polymer Science, 39(1),* 31–42. https://doi.org/10.1002/a1990.070390103
21. Atchudan, R., Edison, T. N. J. I., Perumal, S., Lee, Y. R. (2017). Green synthesis of nitrogen-doped graphitic carbon sheets with use of *Prunus persica* for supercapacitor applications. *Applied Surface Science, 393(30),* 276–286. https://doi.org/10.1016/j.apsusc.2016.10.030
22. Linda, B., Paul, G. (2009). Surface composition and morphology of CTMP fibers. *Holzforschung, 53(2),* 188–194. https://doi.org/10.1515/HF.1999.031

23. Shikha, J. A. I. N., Ankita, J. A. I. N., Kachhawah, P., Devra, V. (2015). Synthesis and size control of copper nanoparticles and their catalytic application. *Transactions of Nonferrous Metals Society of China, 25(12),* 3995–4000. https://doi.org/10.1016/S1003-6326(15)64048-1
24. Wu, C., Mosher, B. P., Zeng, T. (2006). One-step green route to narrowly dispersed copper nanocrystals. *Journal of Nanopartile Research, 8,* 965–969. https://doi.org/10.1007/s11051-005-9065-2
25. Yunlan, M. (2011). *The influence of fibers modified via plasma on the physical properties of paper (Ph.D. Thesis)*. South China University of Technology, Guangzhou, China.
26. Herrera, R., Erdocia, X., Llano-Ponte, R., Labidi, J. (2014). Characterization of hydrothermally treated wood in relation to changes on its chemical composition and physical properties. *Journal of Analytical and Applied Pyrolysis, 107,* 256–266. https://doi.org/10.1016/j.jaap.2014.03.010
27. Li, L., Xie, G., Li, W., Li, Y., Li, X. (2020). The effect of heat treatment on the moisture absorption characteristics of Cu-impregnated masson's pine wood. *BioResources, 15(4),* 8459–8471. https://doi.org/10.15376/biores.15.4.8459-8471
28. Zhao, X., Huang, J., Li, Z., Chen, Y., Müller, M. (2022). Influence of reaction time, temperature, and heavy metal zinc on characteristics of cellulose-and wood-derived hydrochars from hydrothermal carbonization. *BioEnergy Research*. https://doi.org/10.1007/s12155-022-10482-6
29. Lu, X., Ma, X. (2022). Co-hydrothermal carbonization of sewage sludge and bamboo: Hydrochar properties and risk assessment of heavy metals. *Biomass Conversion and Biorefinery.* https://doi.org/10.1007/s13399-022-03223-4
30. Rafique, M., Tahir, M. B., Irshad, M., Nabi, G., Gillani, S. S. A. et al. (2020). Novel *Citrus aurantifolia* leaves based biosynthesis of copper oxide nanoparticles for environmental and wastewater purification as an efficient photocatalyst and antibacterial agent. *Optik, 219,* 165138. https://doi.org/10.1016/j.ijleo.2020.165138
31. He, L., Chen, L., Xiang, L., Liu, H., Shao, H. et al. (2021). Improving the anti-mould property of moso bamboo surface by using a bamboo green colour preservation approach. *Wood Material Science & Engineering*. https://doi.org/10.1080/17480272.2021.2000023
32. Kamdem, D. P., Zhang, J., Freeman, M. H. (1998). The effect of post-streaming on copper naphthenate-treated southern pine. *Wood & Fiber Science, 30,* 210–217.
33. Saranpää, P., Höll, W. (1989). Soluble carbohydrates of *Pinus sylvestris* L. sapwood and heartwood. *Trees, 3(3),* 138–143. https://doi.org/10.1007/BF00226648
34. Kartal, S. N., Hwang, W. J., Imamura, Y. (2008). Combined effect of boron compounds and heat treatments on wood properties: Chemical and strength properties of wood. *Journal of Materials Processing Technology, 198(1–3),* 234–240. https://doi.org/10.1016/j.jmatprotec.2007.07.001
35. Mburu, F., Dumarçay, S., Bocquet, J. F., Petrissans, M., Gérardin, P. (2008). Effect of chemical modifications caused by heat treatment on mechanical properties of *Grevillea robusta* wood. *Polymer Degradation and Stability, 93(2),* 401–405. https://doi.org/10.1016/j.polymdegradstab.2007.11.017